IEEE Open Journal of
Intelligent Transportation
Systems

Received 14 March 2023; revised 26 May 2023; accepted 18 June 2023. Date of publication 21 June 2023; date of current version 28 July 2023.
Digital Object Identifier 10.1109/OJITS.2023.3288396

Signalling Design in Sensor-Assisted mmWave Communications for Cooperative Driving

GIOVANNI CIARAMITARO [1] (Graduate Student Member, IEEE), MATTIA BRAMBILLA [1] (Member, IEEE), MONICA NICOLI [2] (Senior Member, IEEE), AND UMBERTO SPAGNOLINI [1] (Senior Member, IEEE)

[1]Department of Electronics, Information and Bioengineering, Politecnico di Milano, 20133 Milan, Italy

[2]Department of Management, Economics and Industrial Engineering, Politecnico di Milano, 20133 Milan, Italy

CORRESPONDING AUTHOR: G. CIARAMITARO (e-mail: giovanni.ciaramitaro@polimi.it)

This work was supported by the framework of the Huawei-Politecnico di Milano Joint Research Lab.

ABSTRACT Millimeter-Wave (mmWave) Vehicle-To-Vehicle (V2V) communications are a key enabler for connected and automated vehicles, as they support the low-latency exchange of control signals and high-resolution imaging data for maneuvering coordination. The employment of mmWave V2V communications calls for Beam Alignment and Tracking (BAT) procedures to ensure that the antenna beams are properly steered during motion. The conventional beam sweeping approach is known to be unsuited for the high vehicular mobility and its large overhead reduces transmission efficiency. A promising solution to reduce BAT signalling foresees the integration of V2V communication systems with on-board vehicle sensors. We focus on a cooperative sensor-assisted architecture for mmWave V2V communications in line of sight, where vehicles exchange the estimate of antenna position and its uncertainty to compute the optimal beam direction and dimension. We analyze and compare different signalling strategies for sharing the information on the antenna estimate, evaluating the tradeoff between signalling overhead and performance loss for different position and uncertainty encoding strategies. Main attention is given to differential quantization on both the antenna position and uncertainty. Analyses over realistic urban mobility trajectories suggest that differential approaches introduce a negligible performance loss while significantly reducing the BAT signalling communication overhead.

INDEX TERMS Beam pointing, beam tracking, V2V, mmWave, signalling, sensor-assisted communications, beamwidth adaptation.

I. INTRODUCTION

In the recent years, the interest for Connected and Automated Vehicles (CAVs) has been rapidly growing, motivated by the potential gains in terms of road safety and traffic efficiency brought by a synchronized mobility ecosystem [1], [2], [3]. Enhanced Vehicle-To-Everything (V2X) services for CAVs [4] push the design of a Physical (PHY) layer supporting the tight requirements of reliability and low latency, as well as extremely high data rates (1 Gbps) enabling, for instance, cooperative sensing use cases.

Millimeter-Wave (mmWave) V2X communications have been shown to potentially satisfy such rate demand, thanks to massive Multiple-Input Multiple-Output (mMIMO) technologies and large bandwidth availability [5]. They have been introduced in the Fifth Generation (5G) of cellular communications systems under the Cellular V2X (C-V2X) umbrella since Rel. 16 of 3GPP documents [6], [7]. To face the problems of blockage and high path loss [8], especially in vehicular scenarios, mMIMO systems are mandatory and need to guarantee a fast control of the beam pointing from the Transmitter (Tx) to the Receiver (Rx). The smaller the Beam Width (BW) the larger the sensitivity to misalignment errors [9]. Moreover, the topology of the vehicular network constantly changes and the beam pointing needs to be rapidly updated in real time [10].

Conventional solutions for Beam Alignment and Tracking (BAT) in the literature consider an exhaustive search of the

The review of this article was arranged by Associate Editor Alberto Petrillo.

best Tx and Rx beam pair [11]. This procedure is extremely time demanding, especially when a high number of beam pairs needs to be tested, and it is clearly unfeasible with vehicles travelling at high speed or in trajectories including sharp turns and obstacle avoidance maneuvers.

Some first approaches have been proposed to fasten the alignment procedure [12], [13], [14], [15], [16], [17], [18], [19], [20], [21], [22], [23], [24]. Authors of [12], [13], [14] leverage on vehicle traffic information to select the beam pairs; prior knowledge, however, may not be always available. The analysis proposed in [25] suggests the use of Vehicle-To-Infrastructure (V2I) communications to manage the performance decay in terms of packet loss, delay and throughput caused by an increase of CAVs penetration in the scenario. Works in [17], [18], [19] exploit a radar placed on a Road Side Unit (RSU) to track vehicles' motion and accordingly update the beam pointing direction. A similar approach is used in [20], [21] to integrate the motion control of an autonomous vehicle with beam steering, to provide a stable connection with a base station. RSUs are employed for BW and tracking also in [26], where vehicles are divided in groups based on their distance and motion direction. RSUs with imaging capabilities are considered also in [27], [28], which exploit camera and a lidar measurements, respectively, to define the pointing angles of a vehicular network.

V2I-based solutions require the deployment of a dedicated infrastructure and they do not focus on the more challenging Vehicle-To-Vehicle (V2V) communication, where both Tx and Rx are moving. The work in [29] includes the design of a position-assisted V2V link assuming the presence of a reconfigurable intelligent surface. Authors of [30] propose two beam alignment strategies, either refining an initial wide beam, or continuously testing a subset of narrow beams. Rather than checking several pointing directions, other approaches foresee a tight integration of vehicle navigation and communication. Authors of [15], [16] propose to support beam alignment by coupling mmWave with sub-6 GHz V2V communications. In particular, in [16] information concerning the vehicle state (i.e., location and speed) is transmitted in the sub-6 GHz beacons and used by the vehicles to schedule the transmission and select the beam. Lastly, the work in [24] suggests the use of city map or traffic pattern, together with vehicle position estimate, to optimize the sweeping over a non-uniform set of beams.

As main outcome, all the above cited works highlight the importance of an accurate knowledge of the vehicle state in terms of position and, possibly, orientation [31]. Considering the high diffusion of on-board sensors on commercially available vehicles [32], [33] and the increasing trend of automation, exploiting such hardware to provide position information at the PHY layer of the communication appears as the most viable and cost-effective solution. In this direction, the work in [22] proposes to firstly estimate the beam pointing from vehicle positioning sensors and then rely on velocity information to perform beam tracking. The authors of [34], on the other hand, propose to use on-board cameras to select beam pairs and determine the relative coherence time. Cameras are paired with lidar in [35] for detecting and tracking the target vehicle of the V2V communication, but no explicit analysis on the V2V link is included. Beam pointing and tracking can also be driven by inertial sensors mounted at the antenna [36], [37]. The accuracy of sensors' data, however, is still limited by bias that severely affects the overall communication performance. To enhance the quality of the localization, authors of [23] implement a data fusion algorithm that reduces the uncertainty of the vehicle position information and design a cooperative BAT scheme between the communicating vehicles. The results therein included only refer to a simulation of a highway overtaking scenario, reducing the generality of the approach. Authors of [5], [38] use positioning and visual measurements to predict the motion of the receiver and track the beam direction. In [39] location measurements are used to reduce the number of tested beam pairs and speed up the alignment procedure: sensors data are processed to create an area where the Rx is expected to lie and only the beams crossing this area are tested, resulting in a lower overhead. The work in [40] follows a similar approach, adding the computation of an optimal BW to maximize the channel capacity. Enlarging or reducing the beam dimension has been investigated also in [41], [42], [43], [44], [45] where the authors focus on the V2I case. The adaptation of the BW in V2V beam alignment scenario, instead, is considered in [46], where channel and queue state information of the link are exploited. The work in [47] proposes to compute the optimal beam as a function of the mean data-rate. However, the authors do not take into consideration the localization uncertainty for the Rx vehicle (only for the Tx one). Authors of [48] provide a location-based beam alignment and adaptation to optimize the inter-vehicular interference. That work, however, takes into consideration only Global Positioning System (GPS) measurements, without exploiting additional sensors.

We propose a new strategy that allows to exploit the available location information from on-board equipment, combining it with V2V cooperation and data fusion to reduce the uncertainty on the estimate of vehicle state (position and orientation), along with an optimization of the required signalling, thus minimizing the communication overhead. This work is rooted in [49], [50] for what concerns the cooperative Sensor-Assisted (SA) architecture for BAT, whereas the signalling analysis in a 3GPP C-V2X standard context and related optimization is a new original contribution of this paper. We design a parameter exchange strategy to support a cooperative BAT between a pair of vehicles in Line Of Sight (LOS) conditions. In particular, we study different information quantization strategies to disseminate *i*) the antenna position estimate and *ii*) associated uncertainty (i.e., variance). We propose an encoder fully compliant with the existing standards [6], [51], and a differential approach which leverages on the variation of the considered quantities over a communication frame that reduces the signalling overhead.

The proposed SA methodology requires the information of on-board sensors to be available at the PHY layer of V2X communication to implement a BAT procedure. Position-related information is nowadays available at the facility layer of the V2X protocol stack, as it is conveyed, for instance, into Cooperative Awareness Messages (CAM). However, the current dissemination frequency of CAM is prescribed by the current standard up to 10 Hz [52], which does not match the update rate required by a beam steering in high mobility systems. As an example, let us consider two connected vehicles, namely v_1 and v_2, both equipped with an Uniform Planar Array (UPA). Suppose v_1 is transmitting to v_2 with a BW ϕ. The inter-vehicle distance is $d = 20$ m. Assume v_2 is moving in a direction orthogonal to the LOS between v_1 and v_2 with speed $v = 40$ km/h. If the pointing direction of vehicle v_1 does not change, the time T required by vehicle v_2 to exit the coverage area of the beam is $T = d\tan(\phi)/v$. If the UPA has 8 antennas, i.e., $\phi = 12.74$ deg, this time is $T = 120$ ms. If the UPA has twice the number of antennas ($\phi = 6.37$ deg), the time reduces to $T = 60$ ms. This shows that the current CAM update frequency results unsuited for a cooperative beam alignment scheme when extremely narrow beams are employed. To overcome this limitation, we here propose position-related information to be exchanged at the PHY level of a C-V2X protocol. This is not allowed in current V2X communication standard [6], [53], which does not allocate space for such information, meaning that no integration of telecommunication and sensor information is considered at time being. Once the two vehicles are connected, in fact, refinement of Tx and Rx beams are performed through transmission of channel state information messages and sounding reference signals. The latest release of 3GPP C-V2X, namely Rel. 17 [54], introduced a number of novelties (spectrum expansion up to 71 GHz, enhancement of mMIMO system and expansion of sidelink supported band) but signalling of position information at PHY is not considered yet. We show in this work that a modification in this sense would allow for a robust BAT procedure at the cost of a limited overhead and, most notably, would improve the throughput of the V2V link.

The remainder of this paper is organized as follows: Section II describes the V2V channel, SA architecture and the communication hardware to enable BW adaptation. Section III includes the design of signalling strategies of position and covariance information in the V2V link to support SA method. Section IV describes the urban traffic simulations with Simulator of Urban MObility (SUMO) software and the numerical results. Finally Section V draws conclusions of this work.

II. SYSTEM MODEL

This section is devoted to describe the SA architecture, the MIMO antenna models and the performance metrics that will be used to evaluate the designed signalling solutions.

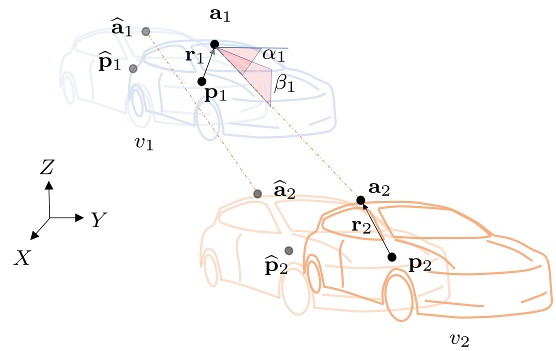

FIGURE 1. V2V system with graphical description of true and estimated vehicle positions ($\mathbf{p}_1$, $\mathbf{p}_2$, $\widehat{\mathbf{p}}_1$ and $\widehat{\mathbf{p}}_2$), true and estimated antenna positions ($\mathbf{a}_1$, $\mathbf{a}_2$, $\widehat{\mathbf{a}}_1$ and $\widehat{\mathbf{a}}_2$), true azimuth and elevation pointing angles α_1 and β_1 for vehicle v_1.

A. SENSOR-ASSISTED BEAM CONTROL

Let us consider a three dimensional (3D) Cartesian Navigation Reference System (NRS), with axes (X, Y, Z), to model the dynamics of the V2V link between two vehicles (v_1 and v_2), as shown in Fig. 1. Vector $\mathbf{p}_v(t) = [p_{v,X}(t)\ p_{v,Y}(t)\ p_{v,Z}(t)]^{\mathrm{T}} \in \mathbb{R}^3$ contains the coordinates of the Centre of Gravity (COG) of vehicle v at time t, whereas $\mathbb{q}_v(t) \in \mathbb{R}^4$ is the quaternion parametrizing vehicle's orientation [55], both referred to NRS. The antenna position is $\mathbf{a}_v(t) = [a_{v,X}(t)\ a_{v,Y}(t)\ a_{v,Z}(t)]^{\mathrm{T}} \in \mathbb{R}^3$, and typically $\mathbf{a}_v(t) \neq \mathbf{p}_v(t)$. In our study, the antennas are placed on the vehicle's roof, according to the 3GPP recommendations in [56]. Assuming the vehicle is a rigid body, the following holds [57]:

$$\mathbf{a}_v(t) = \mathbf{p}_v(t) + \mathbf{R}(\mathbb{q}_v(t))\mathbf{r}_v, \tag{1}$$

where $\mathbf{r}_v \in \mathbb{R}^3$ is a constant vector defining the distance of the antenna with respect to the COG and $\mathbf{R}(\mathbb{q}_v(t)) \in \mathbb{R}^{3\times 3}$ is a rotation matrix that accounts for the instantaneous vehicle orientation $\mathbb{q}_v(t)$, as detailed in [55, eq. (A10)].

We consider the SA architecture in [50], where each vehicle is equipped with a GPS and an Inertial Measurement Unit (IMU). The observations provided by GPS and IMU sensors are fused by means of an Extended Kalman Filter (EKF), designed as in [55] for tracking the vehicle dynamics. The outputs of the EKF are an estimate of vehicle position and orientation, $\widehat{\mathbf{p}}_v(t)$ and $\widehat{\mathbb{q}}_v(t)$, respectively, and the related covariance matrices $\mathbf{C}_v^p(t) \in \mathbb{R}^{3\times 3}$ and $\mathbf{C}_v^{\mathbb{q}}(t) \in \mathbb{R}^{4\times 4}$, respectively. The estimate of the antenna position $\widehat{\mathbf{a}}_v(t)$ is retrieved from $\widehat{\mathbf{p}}_v(t)$ by means of (1). The covariance matrix of $\widehat{\mathbf{a}}_v(t)$, namely $\mathbf{C}_v^a(t) \in \mathbb{R}^{3\times 3}$ is computed as

$$\mathbf{C}_v^a(t) = \mathbf{C}_v^p(t) + \mathrm{Cov}(\mathbf{R}(\widehat{\mathbb{q}}_v(t))\mathbf{r}_v). \tag{2}$$

Since $\mathbf{r}_v$ is deterministic (a vehicle-dependent parameter), the second term in (2) accounts only for the uncertainty on the orientation that typically has a negligible impact with respect to the first one. It follows that $\mathbf{C}_v^a(t) \approx \mathbf{C}_v^p(t)$.

Let us consider the perspective of vehicle v_1, which knows $\widehat{\mathbf{a}}_1(t)$, $\mathbf{C}_1^a(t)$ and $\mathbf{C}_v^{\mathbb{q}}(t)$, and receives $\widehat{\mathbf{a}}_2(t)$ and $\mathbf{C}_2^a(t)$ from vehicle v_2. The following disclosure is also valid for v_2 perspective, with proper adjustments.

The LOS direction is determined by the Tx and Rx antenna positions. In the ideal case of perfect mutual awareness of the positions, the azimuth and elevation pointing angles, $\alpha_1(t)$ and $\beta_1(t)$ respectively, are

$$\alpha_1(t) = \operatorname{atan}\left(\frac{a_{2,Y}(t) - a_{1,Y}(t)}{a_{2,X}(t) - a_{1,X}(t)}\right) = \operatorname{atan}\left(\frac{\Delta a^1_{1,2,Y}(t)}{\Delta a^1_{1,2,X}(t)}\right), \quad \text{(3a)}$$

$$\beta_1(t) = \operatorname{asin}\left(\frac{a_{2,Z}(t) - a_{1,Z}(t)}{\|\mathbf{a}_2(t) - \mathbf{a}_1(t)\|}\right) = \operatorname{asin}\left(\frac{\Delta a^1_{1,2,Z}(t)}{\left\|\Delta \mathbf{a}^2_{1,2}(t)\right\|}\right). \quad \text{(3b)}$$

The pointing directions are collected into vector $\boldsymbol{\xi}_1(t) = [\alpha_1(t)\ \beta_1(t)]$. Since v_1 knows $\widehat{\mathbf{a}}_1(t)$ and $\widehat{\mathbf{a}}_2(t)$, it computes the estimate of the pointing directions $\widehat{\boldsymbol{\xi}}_1(t)$, by means of (3).

The considered SA procedure assumes that v_1 is capable of enlarging or reducing the BW according to the quality of the beam tracking. Intuitively, the more accurate is the estimate of the state of both vehicles, the narrower can be the beam. BW adaptation is performed as described in [50] and it considers the covariance of $\widehat{\xi}_1(t)$ as an indicator of the reliability of the LOS estimate. The covariance of the LOS estimate available at vehicle v_1, i.e, $\mathbf{C}_{\mathrm{LOS},1}(t)$, is obtained from $\mathbf{C}^a_1(t)$, $\mathbf{C}^a_2(t)$ and $\mathbf{C}^{\mathbb{q}}_1(t)$ according to [50, eq. (29)]

$$\mathbf{C}_{\mathrm{LOS},1}(t) = \boldsymbol{\Lambda}\mathbf{C}^{\mathbb{q}}_1(t)\boldsymbol{\Lambda}^{\mathrm{T}} + \mathbf{R}(\mathbb{q}_v(t))\big(\mathbf{C}^a(t)\big)\mathbf{R}(\mathbb{q}_v(t))^{\mathrm{T}}, \quad (4)$$

where $\boldsymbol{\Lambda} = \frac{\partial \mathbf{R}(\mathbb{q}_v(t))}{\partial \mathbb{q}_v(t)}$ and $\mathbf{C}^a(t) = \mathbf{C}^a_1(t) + \mathbf{C}^a_2(t)$. The standard deviations of azimuth and elevation estimates, namely $\sigma^\alpha_1(t)$ and $\sigma^\beta_1(t)$, are computed as

$$\sigma^\alpha_1(t) = \sqrt{\mathbf{b}_{\alpha,1}(t)^{\mathrm{T}}\mathbf{C}_{\mathrm{LOS},1}(t)\mathbf{b}_{\alpha,1}(t)}, \quad \text{(5a)}$$

$$\sigma^\beta_1(t) = \sqrt{\mathbf{b}_{\beta,1}(t)^{\mathrm{T}}\mathbf{C}_{\mathrm{LOS},1}(t)\mathbf{b}_{\beta,1}(t)}, \quad \text{(5b)}$$

where $\mathbf{b}_{\alpha,1}(t) \in \mathbb{R}^{3\times 1}$ and $\mathbf{b}_{\beta,1}(t) \in \mathbb{R}^{3\times 1}$ are the gradients of $\alpha_1(t)$ and $\beta_1(t)$ with respect to $\Delta\mathbf{a}^1_{1,2}(t)$. The azimuth and elevation standard deviations $\sigma^\alpha_1(t)$ and $\sigma^\beta_1(t)$ are used to compute the azimuth and elevation components of optimal BW of vehicle v_1, $\phi^\alpha_1(t)$ and $\phi^\beta_1(t)$ respectively, as

$$\phi^\alpha_1(t) = 2\,k\,\sigma^\alpha_1(t) \quad \text{(6a)}$$

$$\phi^\beta_1(t) = 2\,k\,\sigma^\beta_1(t), \quad \text{(6b)}$$

which cover the $\pm k\sigma$ confidence interval of pointing errors (in this work $k = 3$ to account for 99.7% of cases).

B. MIMO ANTENNA

Each vehicle is assumed to be equipped with two MIMO UPAs, both placed on the roof, one at the front and one at the rear, according to [56]. To simplify the reasoning, the vehicle has the possibility to select one of them at a time, according to the pointing direction. The UPA has $N^{\mathrm{tot}}_{\mathrm{ant}} \times N^{\mathrm{tot}}_{\mathrm{ant}}$ antenna elements overall, half-wavelength spaced. To shape a communication beam with an optimized dynamic BW, we assume a variable number of active antennas $N^{\mathrm{on}}_{\mathrm{ant},v}(t) \leq N^{\mathrm{tot}}_{\mathrm{ant}}$, as shown in Fig. 2. The number of active antennas $N^{\mathrm{on}}_{\mathrm{ant},v}(t)$ determines the BW on both azimuth and elevation (i.e., $\phi^\alpha_v(t)$ and $\phi^\beta_v(t)$). An example of BW control is given in [58].

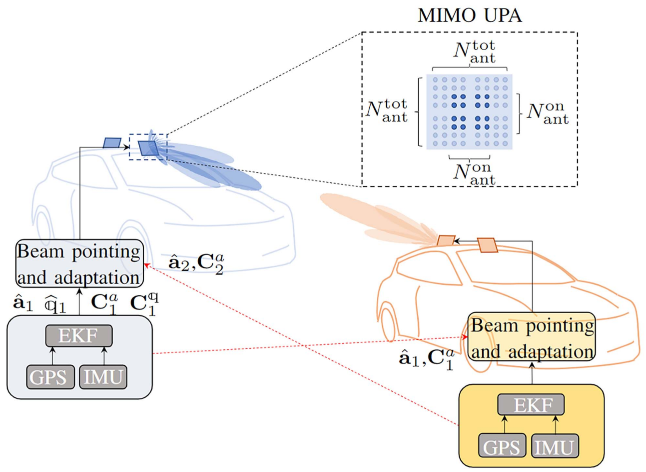

FIGURE 2. **SA beam pointing scheme with BW adaptation using UPAs with controllable number of active antennas.**

Assuming a circular shaped beam, the approach we employ to adapt the BW consists in turning on/off the antennas so that $N^{\mathrm{on}}_{\mathrm{ant},v}(t)$ is the same along the horizontal and vertical array dimension. This introduces the constraint $\phi^\alpha_v(t) = \phi^\beta_v(t) = \phi_v(t)$, i.e., the BW is the same along the azimuth and elevation directions. Considering that the motion of the vehicles mostly happens on the horizontal plane (XY of the NRS), we have $\sigma^\alpha_v(t) > \sigma^\beta_v(t)$, hence $\phi_v(t) = \phi^\alpha_v(t) > \phi^\beta_v(t)$. The relation between the number of active antennas $N^{\mathrm{on}}_{\mathrm{ant},v}(t)$ and $\phi_v(t)$ is as follow [59]

$$\phi_v(t) \approx \frac{1.78}{N^{\mathrm{on}}_{\mathrm{ant},v}(t)\cos(\alpha_v(t))}, \quad (7)$$

where the term $\cos(\alpha_v(t))$ denotes a broadening of $\phi_v(t)$ according to the pointing direction. From (7), the number of active antennas is

$$N^{\mathrm{on}}_{\mathrm{ant},v}(t) = \left\lceil \frac{1.78}{\phi_v(t)\cos(\alpha_v(t))} \right\rceil, \quad (8)$$

setting $\phi_v(t)$ equal to the value computed in (6a), i.e., as function of $\sigma^\alpha_v(t)$. Ceiling function $\lceil\cdot\rceil$ is introduced since $N^{\mathrm{on}}_{\mathrm{ant},v}(t)$ is bounded to integer values.

C. PERFORMANCE METRICS

Moving from the ideal case of Section II-A to a practical V2X system, the knowledge of pointing angles is unavoidably subject to an error $\Delta\boldsymbol{\xi}_v(t) = \widehat{\boldsymbol{\xi}}_v(t) - \boldsymbol{\xi}_v(t)$. This pointing mismatch reduces the antenna gain with respect to the ideal case (i.e., $\Delta\boldsymbol{\xi}_v = [0\ 0]^{\mathrm{T}}$) by a quantity that is computed as in the following. Let the antenna gain associated to the estimated pointing angles be

$$G_v\big(\boldsymbol{\xi}_v(t), \Delta\boldsymbol{\xi}_v(t)\big) = |\mathbf{s}\big((\boldsymbol{\xi}_v(t) + \Delta\boldsymbol{\xi}_v(t))\big)^{\mathrm{H}}\mathbf{s}\big(\boldsymbol{\xi}_v(t)\big)|^2, \quad (9)$$

where $\mathbf{s}((\boldsymbol{\xi}_v(t)+\Delta\boldsymbol{\xi}_v(t)))$ and $\mathbf{s}(\boldsymbol{\xi}_v(t))$ are the steering vectors corresponding to the pointing direction $\boldsymbol{\xi}_v(t)+\Delta\boldsymbol{\xi}_v(t)$ and $\boldsymbol{\xi}_v(t)$, respectively. For a generic pointing direction $\boldsymbol{\xi}_v(t) = [\alpha_v(t)\ \beta_v(t)]^{\mathrm{T}}$, the steering vector is [60]

$$\mathbf{s}_v\big(\boldsymbol{\xi}_v(t)\big) = \begin{bmatrix} e^{-j\frac{2\pi}{\lambda}\boldsymbol{\mu}_1^{\mathrm{T}}\mathbf{w}(\boldsymbol{\xi}_v(t))} \\ e^{-j\frac{2\pi}{\lambda}\boldsymbol{\mu}_2^{\mathrm{T}}\mathbf{w}(\boldsymbol{\xi}_v(t))} \\ \vdots \\ e^{-j\frac{2\pi}{\lambda}\boldsymbol{\mu}_i^{\mathrm{T}}\mathbf{w}(\boldsymbol{\xi}_v(t))} \\ \vdots \\ e^{-\frac{j2\pi}{\lambda}\boldsymbol{\mu}_{N^{\mathrm{on}}_{\mathrm{ant},v(t)}}^{\mathrm{T}}\mathbf{w}(\boldsymbol{\xi}_v(t))} \end{bmatrix}, \tag{10}$$

being $\boldsymbol{\mu}_i \in \mathbb{R}^3$ the position vector of the i-th element of the antenna and $\mathbf{w}(\boldsymbol{\xi}_v(t)) = [\cos(\beta_v(t))\sin(\alpha_v(t))\ \cos(\beta_v(t))\cos(\alpha_v(t))\ \ \sin(\beta_v(t))]^{\mathrm{T}}$ the wave propagation direction along the LOS. In case of perfect pointing, i.e., for $\Delta\boldsymbol{\xi}_v(t) = [0\ 0]^{\mathrm{T}}$, $G_v(\boldsymbol{\xi}_v(t), \mathbf{0}_{2\times 1}) \triangleq G_{\mathrm{id},v}(\boldsymbol{\xi}_v(t))$ is the ideal gain as function of $\boldsymbol{\xi}_v(t)$.

In our analysis we will use the mismatched antenna gain $G_v(\boldsymbol{\xi}_v(t), \Delta\boldsymbol{\xi}_v(t))$ to compute the SNR of the link and thus to assess the performance loss due to pointing errors. Notice that, in the following, we are setting v_1 and v_2 as Tx and Rx respectively, but same procedure applies to the reverse link. The SNR is written, in dB scale, as

$$\begin{aligned}\mathrm{SNR}^{\mathrm{dB}}(t) = P_1^{\mathrm{dB}} &+ G^{\mathrm{dB}}\big(\boldsymbol{\xi}_1(t), \Delta\boldsymbol{\xi}_1(t), \boldsymbol{\xi}_2(t), \Delta\boldsymbol{\xi}_2(t)\big) \\ &- \mathrm{PL}^{\mathrm{dB}}(d(t)) - P_n^{\mathrm{dB}},\end{aligned} \tag{11}$$

where $G^{\mathrm{dB}}(\boldsymbol{\xi}_1(t), \Delta\boldsymbol{\xi}_1(t), \boldsymbol{\xi}_2(t), \Delta\boldsymbol{\xi}_2(t)) = G_1^{\mathrm{dB}}(\boldsymbol{\xi}_1(t), \Delta\boldsymbol{\xi}_1(t)) + G_2^{\mathrm{dB}}(\boldsymbol{\xi}_2(t), \Delta\boldsymbol{\xi}_2(t))$, P_1 is the Tx power, P_n is the noise power at each element of the receiving antenna array of vehicle v_2, $d(t)$ is the distance between the vehicles and $\mathrm{PL}(d(t))$ represents the path loss. The latter is [61]

$$\mathrm{PL}^{\mathrm{dB}}(d(t)) = -147.55 + 10\,\eta\log_{10}(d(t)) + 20\log_{10}(f), \tag{12}$$

where f is the carrier frequency and η is the pathloss exponent. P_n^{dB} is computed as

$$P_n^{\mathrm{dB}} = -204 + 10\log_{10}B + \mathrm{NF}^{\mathrm{dB}}, \tag{13}$$

being $\mathrm{NF}^{\mathrm{dB}}$ the noise floor and B the communication bandwidth.

In case of perfect beam pointing, the ideal SNR is

$$\mathrm{SNR}_{\mathrm{id}}^{\mathrm{dB}}(t) = P_1^{\mathrm{dB}} + G_{\mathrm{id}}^{\mathrm{dB}}\big(\boldsymbol{\xi}_1(t), \boldsymbol{\xi}_2(t)\big) - \mathrm{PL}^{\mathrm{dB}}(d(t)) - P_n^{\mathrm{dB}}, \tag{14}$$

where $G_{\mathrm{id}}^{\mathrm{dB}}(\boldsymbol{\xi}_1(t), \boldsymbol{\xi}_2(t)) = G_{\mathrm{id},1}(\boldsymbol{\xi}_1(t)) + G_{\mathrm{id},2}(\boldsymbol{\xi}_2(t))$. To highlight only the losses associated to misalignment, we define the SNR loss as in (15), shown at the bottom of the page, where the terms related to path loss and noise floor cancel out, since they are equal for both $\mathrm{SNR}^{\mathrm{dB}}(t)$ and $\mathrm{SNR}_{\mathrm{id}}^{\mathrm{dB}}(t)$.

The last two metrics used for performance assessment are *i)* the fading duration F, defined as the time interval in which the SNR persists in outage, i.e., $\mathrm{SNR}(t) < \overline{\mathrm{SNR}}$, with $\overline{\mathrm{SNR}}$ the outage threshold; *ii)* channel capacity C defined as

$$C(t) = B\,\log_2(1 + \mathrm{SNR}(t)) \tag{16}$$

according to Shannon-Hartley theorem.

The adopted metrics focus on the evaluation of the performance degradation caused only by incorrect beam alignment. For this reason, the V2V communication channel is assumed as ideal, neglecting the effects of multipath propagation and encoding/decoding stages.

III. V2V SIGNALLING DESIGN

In this section, we propose multiple strategies to optimize the signalling of the information required by the SA approach with adaptive BW between a pair of connected vehicles, v_1 and v_2, as described above in Section II-A. Recall that the information to be shared by vehicle v is the estimate of the antenna position $\widehat{\boldsymbol{a}}_v \in \mathbb{R}^{3\times 1}$ and the related covariance matrix $\mathbf{C}_v^a(t) \in \mathbb{R}^{3\times 3}$. For the sake of brevity, we describe the signalling from the perspective of vehicle v_1, which receives $\widehat{\mathbf{a}}_2(t)$ and $\mathbf{C}_2^a(t)$ every $\tau = 10$ ms (the duration of a 5G frame [6]). Note that only the quantization and signalling of these quantities related to vehicle v_2 is derived, since $\widehat{\mathbf{a}}_1(t)$ and $\mathbf{C}_1^a(t)$ are assumed to be available at vehicle v_1 at each time instant.

A. SIGNALLING OF POSITION INFORMATION

The dissemination of position information by v_2 allows v_1 to compute $\widehat{\boldsymbol{\xi}}_1(t)$ from (3). For this task, we design two different approaches. In the first one the vehicles share their absolute position estimate, in the second one they only send the variation of the position with respect to the latest available information, with the scope of reducing the signalling overhead.

1) ABSOLUTE POSITION SIGNALLING

The first proposed approach assumes to share $\widehat{\mathbf{a}}_2(t)$, i.e., the antenna position estimate with respect to an absolute spatial reference system. To this aim we employ the WGS84 reference system [62], the standard for encoding absolute position of GPS, which uses $N_{\mathrm{bit}}^{\mathrm{pos}} = 32$ bits for each of the

$$\begin{aligned}\mathrm{SNR}_{\mathrm{loss}}^{\mathrm{dB}}(t) &= \underbrace{\Big(P_1^{\mathrm{dB}} + G^{\mathrm{dB}}\big(\boldsymbol{\xi}_1(t), \Delta\boldsymbol{\xi}_1(t), \boldsymbol{\xi}_2(t), \Delta\boldsymbol{\xi}_2(t)\big) - \mathrm{PL}^{\mathrm{dB}}(d(t)) - P_n^{\mathrm{dB}}\Big)}_{\mathrm{SNR}^{\mathrm{dB}}(t)} - \underbrace{\Big(P_1^{\mathrm{dB}} + G_{\mathrm{id}}^{\mathrm{dB}}\big(\boldsymbol{\xi}_1(t), \boldsymbol{\xi}_2(t)\big) - \mathrm{PL}^{\mathrm{dB}}(d(t)) - P_n^{\mathrm{dB}}\Big)}_{\mathrm{SNR}_{\mathrm{id}}^{\mathrm{dB}}(t)} \\ &= G^{\mathrm{dB}}\big(\boldsymbol{\xi}_1(t), \Delta\boldsymbol{\xi}_1(t), \boldsymbol{\xi}_2(t), \Delta\boldsymbol{\xi}_2(t)\big) - G_{\mathrm{id}}^{\mathrm{dB}}\big(\boldsymbol{\xi}_1(t), \boldsymbol{\xi}_2(t)\big)\end{aligned} \tag{15}$$

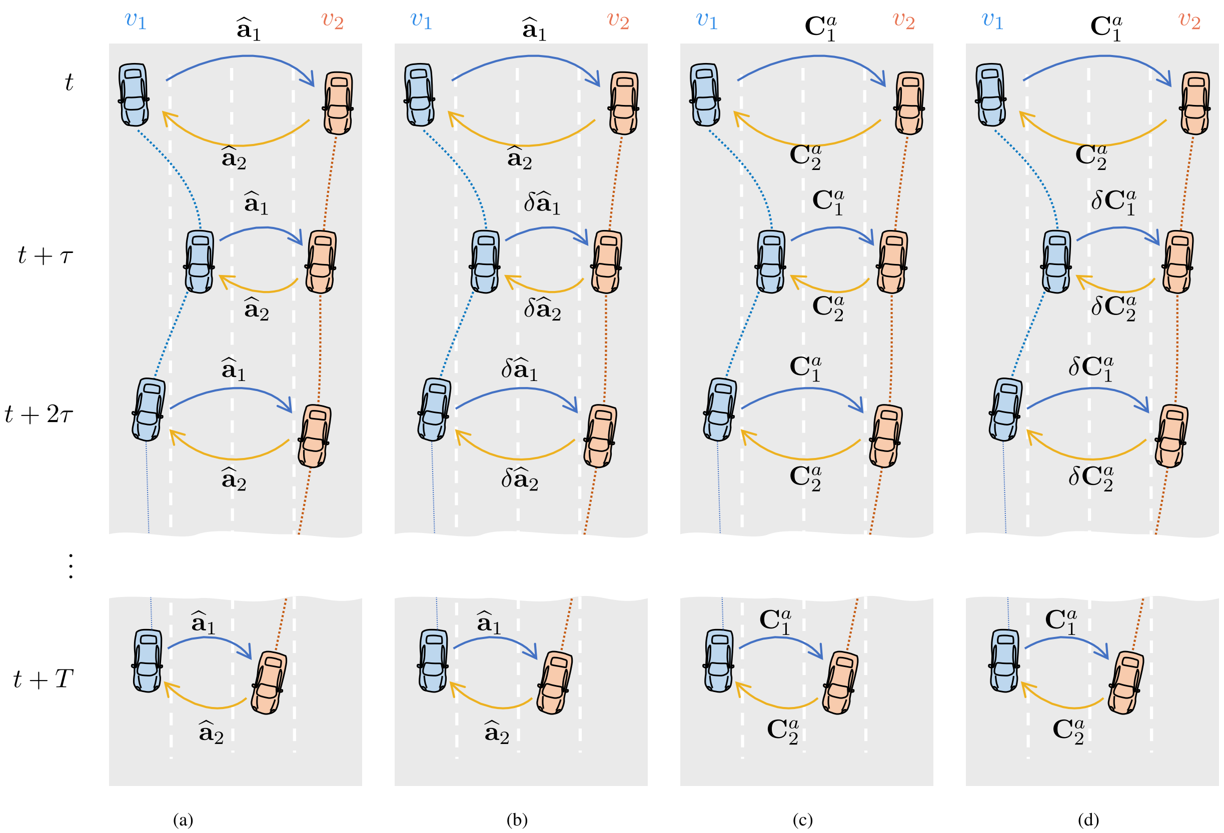

FIGURE 3. Diagram of signalling schemes between vehicles v_1 and v_2. Methods: (a) absolute position; (b) differential position; (c) full covariance; (d) differential covariance.

$n = 3$ position coordinates [62]. For the signalling of $\widehat{\mathbf{a}}_2(t)$, performed with periodicity τ, the required data rate is

$$R^{\text{pos}} = n \cdot \frac{N_{\text{bit}}^{\text{pos}}}{\tau}. \tag{17}$$

Fig. 3a shows the signalling diagram for absolute position information exchange.

2) DIFFERENTIAL POSITION SIGNALLING

To reduce the signalling rate, the second designed approach proposes a differential encoding of position. Consider two consecutive signalling instants, $t-\tau$ and t, and the estimated antenna position vectors of vehicle v_2 in such time instants, i.e., $\widehat{\mathbf{a}}_2(t-\tau)$ and $\widehat{\mathbf{a}}_2(t)$. We propose to signal the variation of the antenna position observed over the elapsed time interval, which we refer to as the differential antenna position $\delta\widehat{\mathbf{a}}_2(t)$, defined as

$$\delta\widehat{\mathbf{a}}_2(t) = \widehat{\mathbf{a}}_2(t) - \widehat{\mathbf{a}}_2(t-\tau) = \begin{bmatrix} \delta\widehat{a}_{2,X}(t) \\ \delta\widehat{a}_{2,Y}(t) \\ \delta\widehat{a}_{2,Z}(t) \end{bmatrix}. \tag{18}$$

This approach leverages on the fact that, once the V2V link is established, v_1 can retrieve the position of the antenna of v_2 at time t based on the last available antenna information, i.e., $\widehat{\mathbf{a}}_2(t) = \widehat{\mathbf{a}}_2(t-\tau) + \delta\widehat{\mathbf{a}}_2(t)$. Note that, in this case, it is necessary to define a suited quantization interval for signalling $\delta\widehat{\mathbf{a}}_2(t)$. To this extent, we consider that current 5G standard [6] is built upon the operability assumption of having vehicles travelling up to $v_{\max} = 250$ km/h. This means that each component of $\delta\widehat{\mathbf{a}}_2(t)$ is assumed to vary less than $v_{\max}\tau = 0.79$ m. We thus conservatively set to ± 1 m the quantization interval for the elements of $\delta\widehat{\mathbf{a}}_2(t)$. The choice of quantization bits $N_{\text{bit}}^{\delta\text{pos}}$ is a tradeoff between the additional error caused by approximation and the communication signalling overhead.

To avoid possible cumulation of errors due to differential encoding, we introduce a periodic signalling of the absolute position $\widehat{\mathbf{a}}_2(t)$ (encoded in $n \cdot N_{\text{bit}}^{\text{pos}}$ bits) after a number of instances of signalling of $\delta\widehat{\mathbf{a}}_2(t)$. Specifically, being τ the periodicity for $\delta\widehat{\mathbf{a}}_2(t)$, we indicate with T the periodicity for $\widehat{\mathbf{a}}_2(t)$ set. We set $T = 1$ s. The required signalling data rate for the differential position approach is

$$R^{\delta\text{pos}} = n \cdot \left(\frac{N_{\text{bit}}^{\delta\text{pos}}}{\tau} + \frac{N_{\text{bit}}^{\text{pos}}}{T} \right), \tag{19}$$

where the first term refers to the signalling of $\delta\widehat{\mathbf{a}}_2$, whereas the second one to the signalling of $\widehat{\mathbf{a}}_2(t)$. According to (19), for $N_{\text{bit}}^{\delta\text{pos}} \in \{3, 6, 10\}$ bit and recalling that $N_{\text{bit}}^{\text{pos}} = 32$, it results that $R_{\text{pos}}^{\text{diff}} \in \{1, 1.9, 3.1\}$ kbps, respectively. Fig. 3b shows the signalling diagram of the differential position information.

TABLE 1. The position confidence and variance levels considered in this work for location covariance signalling.

	Confidence [m]	Variance [m^2]
Level 0	0.1	0.01
Level 1	0.2	0.04
Level 2	0.5	0.25
Level 3	1	1
Level 4	2	4
Level 5	5	25
Level 6	10	100
Level 7	>20	>400

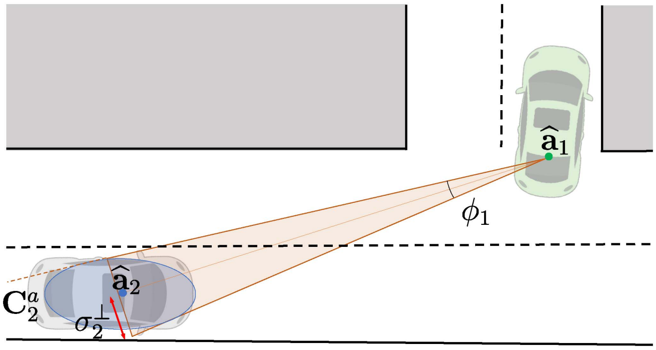

FIGURE 4. Geometrical representation of the scalar covariance $\sigma_2^\perp$, exchanged between vehicles for beam pointing control.

B. SIGNALLING OF LOCATION COVARIANCE INFORMATION

This section discusses the procedures used by vehicle v_2 to share the covariance of antenna position estimate, denoted as

$$\mathbf{C}_2^a(t) = \begin{bmatrix} \sigma^2_{2,XX}(t) & C_{2,XY}(t) & C_{2,XZ}(t) \\ C_{2,YX}(t) & \sigma^2_{2,YY}(t) & C_{2,YZ}(t) \\ C_{2,ZX}(t) & C_{2,ZY}(t) & \sigma^2_{2,ZZ}(t) \end{bmatrix}. \tag{20}$$

Considering the matrix symmetry, univocal representation requires 6 elements. We approximate $\mathbf{C}_v^a(t)$ as a diagonal matrix, assuming that the three position components are uncorrelated, reducing the required elements to $n = 3$.

1) FULL COVARIANCE SIGNALLING

To quantize the values of $\mathbf{C}_2^a(t)$, we rely on the 16 confidence values defined by the SAE standard in [51]. The interval of position confidence values ranges from 0.01 m to 500 m according to a non-uniform quantization. Considering that for beam-based V2V communications it is not attractive to consider the upper and lower values, we limit the confidence values to eight levels, as reported in Table 1, thus requiring $N_{\text{bit}}^{\text{cov}} = 3$ bits for each diagonal entry. The rationale behind our choice is that confidence values larger than 20 m are useless for an accurate beam pointing with narrow beam, and values lower than 10 cm are not achievable for current vehicle navigation and tracking algorithms. Confidence values are then squared, to retrieve the values of variance of $\mathbf{C}_v^a(t)$ reported in the third column of Tab. 1. The covariance signalling data rate of this approach with τ periodicity is

$$R_{\text{cov}} = n \cdot \frac{N_{\text{bit}}^{\text{cov}}}{\tau}. \tag{21}$$

Fig. 3c shows the diagram for the exchange of full covariance information.

2) DIFFERENTIAL COVARIANCE SIGNALLING

Similarly to the position case, to reduce the signalling overhead we propose to quantize the differential covariance as

$$\delta\mathbf{C}_2^a(t) = \text{diag}\Big(\mathbf{C}_2^a(t)\Big) - \text{diag}\Big(\mathbf{C}_2^a(t-1)\Big)$$

$$= \begin{bmatrix} \delta C^a_{2,X}(t) \\ \delta C^a_{2,Y}(t) \\ \delta C^a_{2,Z}(t) \end{bmatrix}, \tag{22}$$

where diag$(\cdot)$ operator extracts the diagonal elements of a square matrix as for (20). Each entry of $\delta\mathbf{C}_2^a(t)$ is encoded with $N_{\text{bit}}^{\delta\text{cov}} = 2$ bits, indicating a relative jump on the quantization levels in Tab. 1 with respect to the previously available information. Similarly, to avoid error cumulation, periodic exchange every T of the full covariance information (encoded in $n \cdot N_{\text{bit}}^{\text{cov}}$ bits) is introduced. The required signalling data rate for the differential covariance approach is

$$R^{\delta\text{cov}} = n \cdot \left(\frac{N_{\text{bit}}^{\delta\text{cov}}}{\tau} + \frac{N_{\text{bit}}^{\text{cov}}}{T}\right). \tag{23}$$

Fig. 3d shows the signalling diagram for differential covariance exchange.

3) SCALAR COVARIANCE SIGNALLING

As final approach, we propose a method which reduces the covariance information to a single scalar value. The underlying motivation is on the higher uncertainty on the plane where vehicle motion occurs (i.e., $\sigma_v^\alpha(t) > \sigma_v^\beta(t)$). This condition allows to signal only the covariance of the LOS azimuth $\sigma_2^\perp(t)$, which is the component of $\mathbf{C}_2^a(t)$ orthogonal to the azimuth LOS direction, as shown in Fig. 4. Denoting the versor of the direction orthogonal to the azimuth as $\mathbf{u}_2^\perp(t) = [\cos(\alpha_2(t))\ \ \sin(\alpha_2(t))\ \ 0]^{\mathrm{T}}$, $\sigma_2^\perp(t)$ is computed as

$$\sigma_2^\perp(t) = \text{Cov}\Big(\mathbf{u}_2^\perp(t)^{\mathrm{T}}\Delta\widehat{\mathbf{a}}(t)\Big) = \mathbf{u}_2^\perp(t)^{\mathrm{T}}\mathbf{C}_2^a(t)\mathbf{u}_2^\perp(t). \tag{24}$$

Quantization of $\sigma_2^\perp(t)$ is the same of the differential covariance, for this reason also in this case we introduce the exchange of $\mathbf{C}_2^a(t)$ with a higher periodicity T. For this last method, the required signalling data rate is

$$R^{\text{scalar cov}} = \frac{N_{\text{bit}}^{\delta\text{cov}}}{\tau} + \frac{N_{\text{bit}}^{\text{cov}}}{T}. \tag{25}$$

To conclude this section on the designed signalling strategies to support SA architecture, we provide in Tab. 2 a summary of the required data rate for all presented methods, computed according to (17), (19), (21) and (23) and

TABLE 2. Required signalling for different methods assuming $N_{\text{bit}}^{\delta\text{pos}} = 6$ bit, $\tau = 10$ ms and $T = 1$ s.

Method	Signalling [kbps]		
	Pos.	Cov.	Tot.
Abs. pos. (Fixed BW)	9.6	-	9.6
Diff. pos. (Fixed BW)	1.9	-	1.9
Full cov. (Adapt. BW)	1.9	0.9	2.8
Diff. cov. (Adapt. BW)	1.9	0.6	2.5
Scalar cov. (Adapt. BW)	1.9	0.2	2.1

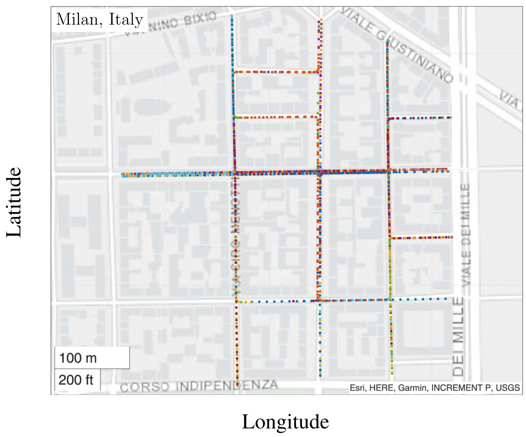

FIGURE 5. Simulated trajectories, colors refer to different vehicles.

TABLE 3. Parameters of the simulation.

Parameter	Value
Environment	
Simulated time	57 s
Sampling time	1 ms
Road class (ISO 8608)	C
Vehicles' pairs	61
Vehicle properties	
Mass	1300 kg
Wheelbase	3.5 m
Track	1.5 m
On-board sensors measurement error (std)	
Position (GNSS)	1 m
Speed (GNSS)	0.1 m/s
Heading (GNSS)	0.3 deg
Acceleration (IMU)	$0.01\ \text{m/s}^2$
Angular rate (IMU)	0.1 rad/s
Communication	
Carrier frequency f	30 GHz
Bandwidth B	400 MHz
Noise floor NF^{dB}	6 dB
Path loss exponent η	2
Latency	10 ms
Outage threshold $\overline{\text{SNR}}$	10 dB

considering $N_{\text{bit}}^{\delta\text{pos}} = 6$ bit, $\tau = 10$ ms and $T = 1$ s. Notice that methods that do not allow adaptation of the BW do not include covariance information exchange.

IV. SIMULATIONS AND RESULTS

This section presents an analysis of the performance of the designed SA signalling strategies, to evaluate the impact of the information encoding (i.e., location and related accuracy) on V2V communication, in terms of link quality (i.e., the SNR loss due to quantization), transmission capacity and robustness to fading. The simulations are performed using realistic planar trajectories generated with Simulator of Urban MObility (SUMO) software, considering an urban area in Milan, Italy, and the framework described in [63] to model the effect of road roughness on vehicle position and orientation, according to ISO 8608 [64]. The resulting 3D vehicle dynamics affect the time evolution of antennas' positions and orientations, which are used to simulate the V2V link.

A. SIMULATION SETTINGS

The simulated urban environment includes 61 pairs of vehicles with trajectories around the Leonardo campus of the Politecnico di Milano, as shown in Fig. 5. Each pair of V2V connected vehicles is simulated with a headway of 5 s between the leader and the follower. With this gap the inter vehicular distance ranges from 10 m to 80 m, with mean value of 37 m. The speed of the vehicles is comprised between 0 km/h and 61.2 km/h, with an average value of 28.8 km/h.

The connected vehicles perform beam alignment with the SA architecture described in Section II-A, exchanging their position estimate and associated accuracy with periodicity τ. The optimal BW, computed as in (6), determines the number of active antennas, by means of (8). Then, each vehicle keeps the pointing angles and the BW constant, until it receives a new position and accuracy information (after a period τ).

The communication parameters f, B, NF^{dB} and the latency are compliant with the 5G V2X standard, whereas $\eta = 2$ assumes free space propagation. Notice that we are considering the largest bandwidth prescribed by the standard for mmWave, i.e., $B = 400$ MHz [6]. The latency quantifies the time interval between the transmission and reception of the position and covariance information among two connected vehicles. The dimensions of vehicles and the performance of on-board sensors are instead consistent with commercially available private vehicles. All the parameters are summarized in Tab. 3.

To show the benefits brought by the proposed signalling strategies, a comparison with a fixed BW BAT procedure relying on currently-available CAM is considered, where vehicles broadcast the ego-antenna position estimate every $\tau_{\text{CAM}} = 100$ ms [65]. The position information is encoded

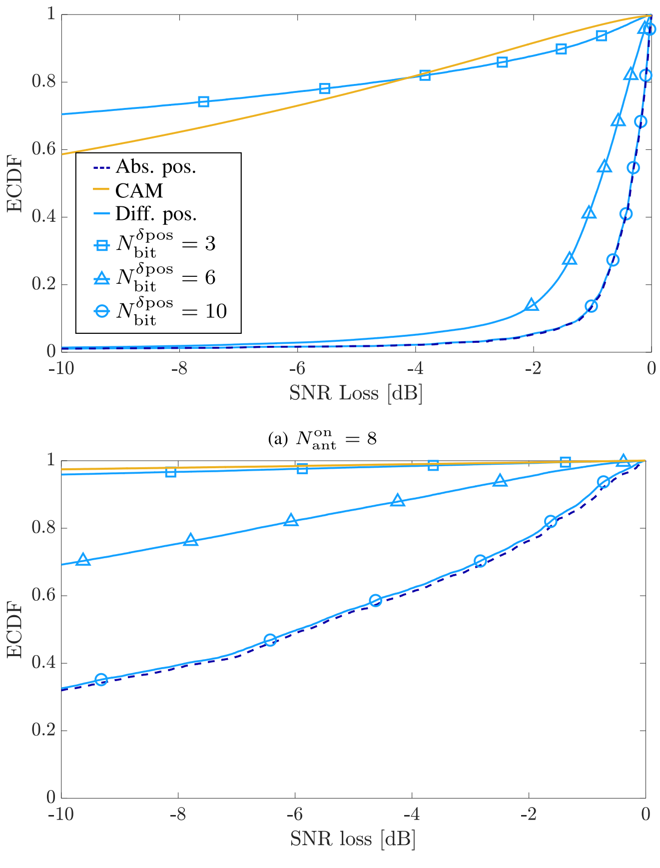

(a) $N_{\mathrm{ant}}^{\mathrm{on}} = 8$

(b) $N_{\mathrm{ant}}^{\mathrm{on}} = 32$

FIGURE 6. Cumulative distribution of SNR loss of fixed beamwidth methods. (a) $N_{\mathrm{ant}}^{\mathrm{on}} = 8$. (b) $N_{\mathrm{ant}}^{\mathrm{on}} = 32$.

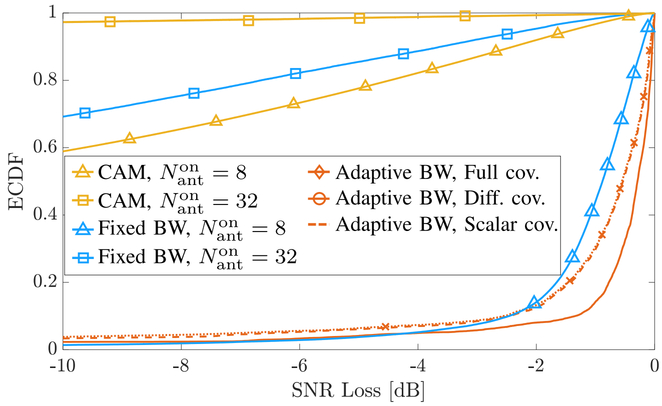

FIGURE 7. Cumulative distribution of SNR loss for fixed and adaptive BW methods.

according to the WGS84 standard [66], hence the CAM-based BAT is equivalent to the absolute position signalling with τ_{CAM} periodicity.

B. IMPACT OF POSITION QUANTIZATION

The first assessment investigates the effect of position information quantization on the SA communication performances using the signalling strategies described in Section III-A. We employ the differential position approach and evaluate its performance with respect to the absolute position one. Three different values of $N_{\mathrm{bit}}^{\mathrm{pos}}$ are considered for differential position encoding. To focus on the impact of position quantization, the first analysis considers a time-invariant number of active antennas $N_{\mathrm{ant},v}^{\mathrm{on}}$, i.e., fixed BW is considered without sharing of covariance information. In Fig. 6 we show the Empirical Cumulative Distribution Function (ECDF) of the SNR loss (15) for $N_{\mathrm{ant},v}^{\mathrm{on}} = 8$ (Fig. 6a) and $N_{\mathrm{ant},v}^{\mathrm{on}} = 32$ (Fig. 6b), which correspond to a fixed BW of $\phi_v = 12.8$ deg and $\phi_v = 3.2$ deg at broadside, respectively. Comparing the two figures, it emerges that CAM-based position dissemination is not suited to support V2V communications over narrow beams. For $N_{\mathrm{ant},v}^{\mathrm{on}} = 8$ (Fig. 6a) and $N_{\mathrm{ant},v}^{\mathrm{on}} = 32$ (Fig. 6b) the SNR loss is higher than the one of SA methods that employ at least $N_{\mathrm{bit}}^{\mathrm{pos}} = 6$ for differential position encoding. The reason for this, as explained by the example in Section I, is the low dissemination rate (10 Hz) of CAM, which is unsuited for highly-dynamic V2V scenarios. Focusing on the proposed method, instead, it can be seen that the additional losses introduced by differential position exchange are higher for $N_{\mathrm{ant},v}^{\mathrm{on}} = 32$ with respect to $N_{\mathrm{ant},v}^{\mathrm{on}} = 8$. This difference is explained considering that the pointing error has a stronger impact on the communication performance when a narrower BW is employed. Focusing on Fig. 6a, the maximum distance between the curves for $N_{\mathrm{bit}}^{\mathrm{pos}} = 6$ and $N_{\mathrm{bit}}^{\mathrm{pos}} = 10$ is in the order of 1 dB and the $N_{\mathrm{bit}}^{\mathrm{pos}} = 10$ case is superimposed to the one employing absolute position. In Fig. 6b, on the other hand, the gap between $N_{\mathrm{bit}}^{\mathrm{pos}} = 6$ and $N_{\mathrm{bit}}^{\mathrm{pos}} = 10$ increases and the latter is no longer superimposed to the absolute position case, although the gap is almost negligible (0.1 dB). We can conclude that, as the BW reduces (e.g., for $N_{\mathrm{ant},v}^{\mathrm{on}} = 32$), the performance is more sensitive to the quantization errors and a higher signalling overhead is required.

C. IMPACT OF COVARIANCE QUANTIZATION

For the analysis on the covariance signalling, we compare the performances of the different strategies described in Section III-B: the full covariance signalling, the differential one and the scalar covariance. For the following analyses, we employ the differential strategy for position encoding. Observing that, introducing BW adaptation, the SA architecture rarely relies on the full MIMO hardware, we select $N_{\mathrm{bit}}^{\mathrm{pos}} = 6$, which is a good trade-off to limit the overhead and the quantization errors. Further details concerning this aspect are given in the next paragraphs.

Fig. 7 shows the SNR loss of two fixed BW methods, with $N_{\mathrm{ant}}^{\mathrm{on}} = 8$ and $N_{\mathrm{ant}}^{\mathrm{on}} = 32$ respectively, and three adaptive BW methods, employing full, differential and scalar covariance signalling. The position signalling is performed with the differential approach and $N_{\mathrm{bit}}^{\mathrm{pos}} = 6$, both for the fixed and adaptive BW methods. We first observe that the additional losses introduced by the differential signalling of the covariance are lower than 1 dB. This is a promising result since the required signalling for the covariance

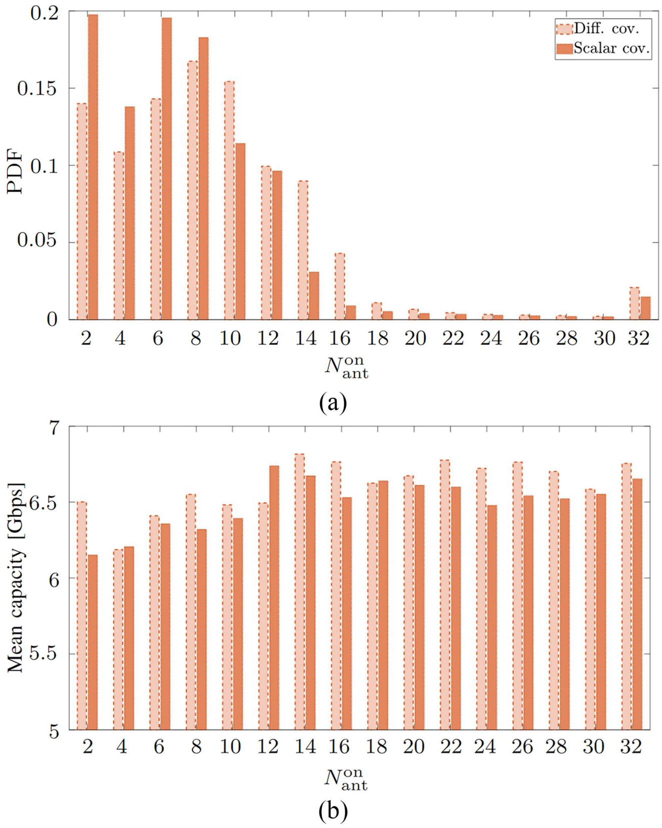

FIGURE 8. Effect of beamwidth adaptation: (a) distribution of selected active antennas; (b) mean capacity guaranteed by the active antennas.

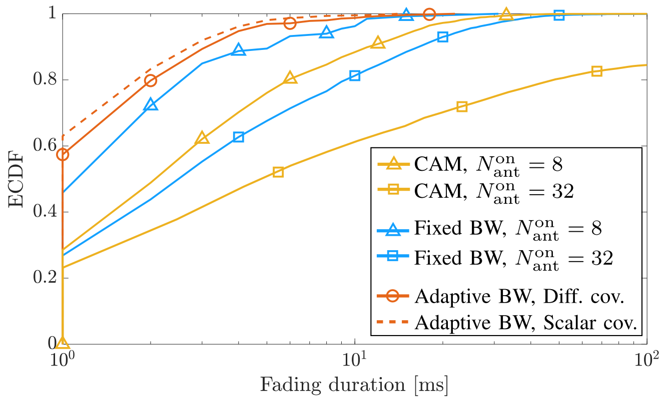

FIGURE 9. Cumulative distribution of fading duration for fixed and adaptive BW methods.

information is halved with respect to the full covariance approach. Secondly, the results highlight the improvements brought by the BW optimization, which, thanks to the covariance signalling, ensures better communication performances with respect to the fixed BW case. The final remark concerns the scalar covariance signalling. The dashed red curve is almost superimposed to the one of the differential covariance, hence no significant differences in terms of SNR loss can be noticed between the two methods. This confirms that the terms that are neglected when exchanging the scalar covariance are not relevant for the proposed BW adaptation.

To deepen the analysis, in Fig. 8 we report the distribution of the number of selected active antennas differential and scalar covariance signalling methods. We notice that scalar covariance is more conservative with respect to the full covariance one, since it tends to select a smaller number of active antennas. This behaviour is explained considering that $\min(\sigma_{XX,v}(t), \sigma_{YY,v}(t)) \leq \sigma_v^{\perp}(t) \leq \max(\sigma_{XX,v}(t), \sigma_{YY,v}(t))$. When $\sigma_{XX,v}(t)$ and $\sigma_{YY,v}(t)$ are encoded with consecutive variance levels of Table 1 (e.g., 0.5 m and 1 m), the uncertainty region of the scalar covariance approach is a circle whose radius coincides with the major semi-axis of the original ellipse. The area where vehicle v is expected to lie leads to the selection of a wider beam (i.e., less active antennas). However, we would like to remark that the reduced number of active antennas does not imply a lower V2V capacity. To prove this, in Fig. 8b we plot the mean capacity versus the number of active antennas. We notice that, overall, the capacity is pretty stable around 6.5 Gbps. It follows that BW adaptation ensures a stable V2V link, which automatically adapts the BW to the uncertainty of antenna information and V2V distance. As a further benchmark, we remark that the average capacity for the fixed BW methods with 8 and 32 active antennas is of 6.5 Gbps and 5.6 Gbps, respectively. This suggests that the current accuracy of vehicle positioning hinders the potential of the MIMO system with a high number of fixed antennas (i.e., narrow beams), as pointing errors introduce significant losses on the MIMO gain.

Besides a reduction of the SNR loss, the adaptive methods ensure better performances also in terms of stability, evaluated with the fading duration. Fig. 9 shows the ECDFs of the fading duration for the considered SA methods and the CAM-based BAT one. The latter is confirmed to be unable to guarantee reliable V2V communication, especially for narrow beams. For $N_{\mathrm{ant}}^{\mathrm{on}} = 32$, the duration of fading when CAM signalling is used is above 10 ms in 40% of the cases. Adaptive methods guarantee a fading below 3 ms in 95% of the cases, whereas the fixed BW ones do not provide such good results, with a fading duration larger than 10 ms in 95% of the cases, which does not meet the requirements of autonomous driving [4].

A final comparison between fixed and adaptive BW methods regards the channel capacity. Fig. 10 reports the ECDF of channel capacity, highlighting that the use of a fixed BW with $N_{\mathrm{ant},v}^{\mathrm{on}} = 8$ guarantees higher stability of the channel, with a capacity always larger than 5 Gbps but bounded to a maximum of 8 Gbps. On the other hand, with $N_{\mathrm{ant},v}^{\mathrm{on}} = 32$, a higher antenna gain is experienced and a larger maximum capacity (9 Gbps) is ensured but, at the same time, it has an extremely high sensitivity to pointing error that makes this option unsuitable to satisfy the V2V communication constraints [4]. Adaptive BW methods combine link stability and capacity, by adjusting dynamically the BW. These results on the impact of covariance quantization on the communication performance suggest that, rather than devoting

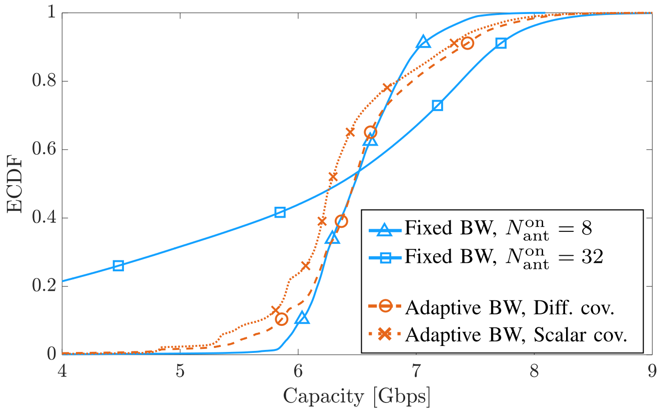

FIGURE 10. Cumulative distribution of V2V channel capacity for fixed and adaptive BW methods.

a large number of bits for position signalling, it is advisable to enable BW optimization through the dissemination of covariance information, especially considering that the additional overhead of the proposed method is in the order of decimals of kbps.

The results included in this section are consistent with the state-of-the art ones. The SNR loss shown in Fig. 6 is comparable to the one included in [45], where the misalignment causes a loss below 3 dB in 95% of the cases. The same statistics is valid for the SA methods proposed in this work, provided that $N^{\mathrm{pos}}_{\mathrm{bit}} \geq 6$. Similarly to the results in [67], the designed BW adaptation is capable of managing extremely narrow beams ($N^{\mathrm{on}}_{\mathrm{ant},v}(t) = 32$, $\phi_v = 3.2$ deg), but without the computational burden of an optimization algorithm. Focusing on the link capacity, the values achieved by the proposed BAT methods are compatible with the findings in [46], provided that the bandwidth is scaled (we used a $B = 400$ MHz instead of 2.16 GHz).

V. CONCLUSION

This paper proposed a number of signalling strategies to support the introduction of SA beam pointing control for mmWave V2V communications. The considered cooperative BAT architecture requires V2V sharing of the estimate of antenna position and its covariance, to track the LOS direction and adapt the dimension of the beam according to the quality of the pointing information. The proposed strategies are evaluated on a realistic simulated urban scenario. The results show that, by exploiting differential approaches for both the position and covariance encoding, the V2V communication system achieves performances compliant with CAV requirements, with moderate signalling overhead. Furthermore we highlighted the importance of adopting a reconfigurable adaptive hardware to cope with the time varying uncertainty of the link estimate. The BW adaptation, indeed, provides a more stable communication with respect to the fixed BW case, at the cost of few kbps of additional signalling.

Future developments will concern the extension of the number of on-board sensors to enhance the accuracy of the pose estimation and better exploit the capabilities of the MIMO system, by employing smaller BW dimensions for a longer time. Moreover, we will consider a more complex scenario, modelling a larger vehicular network, where it is mandatory to model the effects of multipath propagation, interference and inter-vehicular blockage.

ACKNOWLEDGMENT

The authors would like to thank Alberto Perotti of Huawei Technologies Sweden for the collaboration during the development of the project.

REFERENCES

[1] H. Zhou, W. Xu, J. Chen, and W. Wang, "Evolutionary V2X technologies toward the Internet of Vehicles: Challenges and opportunities," *Proc. IEEE*, vol. 108, no. 2, pp. 308–323, Feb. 2020.
[2] S. Aoki and R. Rajkumar, "Safe intersection management with cooperative perception for mixed traffic of human-driven and autonomous vehicles," *IEEE Open J. Veh. Technol.*, vol. 3, pp. 251–265, Jun. 2022. [Online]. Available: https://ieeexplore.ieee.org/document/9789256
[3] G. N. Bifulco, A. Coppola, A. Petrillo, and S. Santini, "Decentralized cooperative crossing at unsignalized intersections via vehicle-to-vehicle communication in mixed traffic flows," *J. Intell. Transp. Syst.*, pp. 1–26, Sep. 2022. [Online]. Available: https://www.tandfonline.com/doi/full/10.1080/15472450.2022.2124868
[4] "5G; service requirements for enhanced V2X scenarios," ETSI, Sophia Antipolis, France, ETSI TS 122 186 v16.2.0, Nov. 2020.
[5] J. Choi, V. Va, N. Gonzalez-Prelcic, R. Daniels, C. R. Bhat, and R. W. Heath, "Millimeter-wave vehicular communication to support massive automotive sensing," *IEEE Commun. Mag.*, vol. 54, no. 12, pp. 160–167, Dec. 2016.
[6] "3rd generation partnership project; technical specification group services and system aspects; release 16 description; summary of Rel-16 work items (release 16)," 3GPP, Sophia Antipolis, France, 3GPP TR 21.916 V16.0.1, Sep. 2021.
[7] M. H. C. Garcia et al., "A tutorial on 5G NR V2X communications," *IEEE Commun. Surveys Tuts.*, vol. 23, no. 3, pp. 1972–2026, 3rd Quart., 2021.
[8] M. Giordani, M. Rebato, A. Zanella, and M. Zorzi, "Coverage and connectivity analysis of millimeter wave vehicular networks," *Ad Hoc Netw.*, vol. 80, pp. 158–171, Nov. 2018.
[9] Y. Pu, F. Wen, and S. Zhou, "Impact of perception errors on sensing assisted vehicle-to-vehicle communications," in *Proc. IEEE/CIC Int. Conf. Commun. China (ICCC Workshops)*, Aug. 2022, pp. 257–262.
[10] K. Zrar Ghafoor et al., "Millimeter-wave communication for Internet of Vehicles: Status, challenges, and perspectives," *IEEE Internet Things J.*, vol. 7, no. 9, pp. 8525–8546, Sep. 2020.
[11] "*IEEE Standard for Information Technology–Telecommunications and Information Exchange Between Systems–Local and Metropolitan Area Networks–Specific Requirements-Part 11: Wireless LAN Medium Access Control (MAC) and Physical Layer (PHY) Specifications Amendment 3: Enhancements For Very High Throughput in the 60 GHz Band*," IEEE Standard 628, Dec. 2012.
[12] A. Mazin, M. Elkourdi, and R. D. Gitlin, "Accelerating beam sweeping in mmWave Standalone 5G new radios using recurrent neural networks," in *Proc. IEEE 88th Veh. Technol. Conf. (VTC-Fall)*, Sep. 2018, pp. 1–4.
[13] Z. L. Fazliu, F. Malandrino, C. F. Chiasserini, and A. Nordio, "MmWave beam management in urban vehicular networks," *IEEE Syst. J.*, vol. 15, no. 2, pp. 2798–2809, Jun. 2021.
[14] D. Wu, Y. Zeng, S. Jin, and R. Zhang, "Environment-aware and training-free beam alignment for mmWave massive MIMO via channel knowledge map," in *Proc. IEEE Int. Conf. Commun. Workshops (ICC Workshops)*, Jun. 2021, pp. 1–7.
[15] T. Nitsche, A. B. Flores, E. W. Knightly, and J. Widmer, "Steering with eyes closed: Mm-wave beam steering without in-band measurement," in *Proc. IEEE Conf. Comput. Commun. (INFOCOM)*, Apr. 2015, pp. 2416–2424.

[16] B. Coll-Perales, J. Gozalvez, and M. Gruteser, “Sub-6GHz assisted MAC for millimeter wave vehicular communications,” *IEEE Commun. Mag.*, vol. 57, no. 3, pp. 125–131, Mar. 2019.

[17] F. Liu, W. Yuan, C. Masouros, and J. Yuan, “Radar-assisted predictive beamforming for vehicular links: Communication served by sensing,” *IEEE Trans. Wireless Commun.*, vol. 19, no. 11, pp. 7704–7719, Nov. 2020.

[18] N. González-Prelcic, R. Méndez-Rial, and R. W. Heath, “Radar aided beam alignment in mmWave V2I communications supporting antenna diversity,” in *Proc. Inf. Theory Appl. Workshop (ITA)*, Mar. 2016, pp. 1–7.

[19] A. Ali, N. González-Prelcic, and A. Ghosh, “Passive radar at the roadside unit to configure millimeter wave vehicle-to-infrastructure links,” *IEEE Trans. Veh. Technol.*, vol. 69, no. 12, pp. 14903–14917, Dec. 2020.

[20] B. Chang, X. Yan, L. Zhang, Z. Chen, L. Li, and M. A. Imran, “Joint communication and control for mmWave/THz beam alignment in V2X networks,” *IEEE Internet Things J.*, vol. 9, no. 13, pp. 11203–11213, Jul. 2022.

[21] K. Gatsis, A. Ribeiro, and G. J. Pappas, “State-based communication design for wireless control systems,” in *Proc. IEEE 55th Conf. Decis. Control (CDC)*, Dec. 2016, pp. 129–134.

[22] K. Kim, J. Song, J.-H. Lee, S.-H. Hyun, and S.-C. Kim, “Robust beam management in position and velocity aware V2V communications using distributed antenna subarrays,” *IEEE Trans. Veh. Technol.*, vol. 71, no. 11, pp. 11703–11716, Nov. 2022.

[23] C. Mahabal, H. Wang, and H. Fang, “Dual mode localization assisted beamforming for mmWave V2V communication,” *IEEE Trans. Veh. Technol.*, vol. 71, no. 9, pp. 9450–9459, Sep. 2022.

[24] M. Mizmizi et al., “Fastening the initial access in 5G NR sidelink for 6G V2X networks,” *Veh. Commun.*, vol. 33, Jan. 2022, Art. no. 100402.

[25] Z. Khan, S. M. Khan, M. Chowdhury, M. Rahman, and M. Islam, “Performance evaluation of 5G millimeter-wave-based vehicular communication for connected vehicles,” *IEEE Access*, vol. 10, pp. 31031–31042, Mar. 2022.

[26] I. Rasheed, F. Hu, Y.-K. Hong, and B. Balasubramanian, “Intelligent vehicle network routing with adaptive 3D beam alignment for mmWave 5G-based V2X communications,” *IEEE Trans. Intell. Transp. Syst.*, vol. 22, no. 5, pp. 2706–2718, May 2021.

[27] M. Alrabeiah, A. Hredzak, and A. Alkhateeb, “Millimeter wave base stations with cameras: Vision-aided beam and blockage prediction,” in *Proc. IEEE 91st Veh. Technol. Conf. (VTC-Spring)*, May 2020, pp. 1–5.

[28] S. Jiang, G. Charan, and A. Alkhateeb, “LiDAR aided future beam prediction in real-world Millimeter wave V2I communications,” *IEEE Wireless Commun. Lett.*, vol. 12, no. 2, pp. 212–216, Feb. 2023.

[29] X. Zheng, W. Cheng, and J. Wang, “Position-aided on/off states judgment for 1-bit RIS assisted V2V mmWave communication,” in *Proc. IEEE Global Commun. Conf.*, Dec. 2022, pp. 3211–3216.

[30] L. Montero, C. Ballesteros, C. de Marco, and L. Jofre, “Beam management for vehicle-to-vehicle (V2V) communications in millimeter wave 5G,” *Veh. Commun.*, vol. 34, Apr. 2022, Art. no. 100424.

[31] R. Di Taranto, S. Muppirisetty, R. Raulefs, D. Slock, T. Svensson, and H. Wymeersch, “Location-aware communications for 5G networks: How location information can improve scalability, latency, and robustness of 5G,” *IEEE Signal Process. Mag.*, vol. 31, no. 6, pp. 102–112, Nov. 2014.

[32] J. Van Brummelen, M. O’Brien, D. Gruyer, and H. Najjaran, “Autonomous vehicle perception: The technology of today and tomorrow,” *Transp. Res. C Emerg. Technol.*, vol. 89, pp. 384–406, Apr. 2018.

[33] J. Guerrero-Ibáñez, S. Zeadally, and J. Contreras-Castillo, “Sensor technologies for intelligent transportation systems,” *Sensors*, vol. 18, no. 4, p. 1212, 2018.

[34] W. Xu, F. Gao, X. Tao, J. Zhang, and A. Alkhateeb, “Computer vision aided mmWave beam alignment in V2X communications,” *IEEE Trans. Wireless Commun.*, vol. 22, no. 4, pp. 2699–2714, Apr. 2023.

[35] H. Ngo, H. Fang, and H. Wang, “Beamforming and scalable image processing in vehicle-to-vehicle networks,” *J. Signal Process. Syst.*, vol. 94, no. 5, pp. 445–454, Jan. 2022.

[36] M. Brambilla, M. Nicoli, S. Savaresi, and U. Spagnolini, “Inertial sensor aided mmWave beam tracking to support cooperative autonomous driving,” in *Proc. IEEE Int. Conf. Commun. Workshops (ICC Workshops)*, May 2019, pp. 1–6.

[37] U. Spagnolini, M. B. Nicoli, M. Brambilla, S. M. Savaresi, and G. Panzani, “Method and system for pointing electromagnetic signals emitted by moving devices,” U.S. Patent 17 440 965, Jun. 2022.

[38] I. Mavromatis, A. Tassi, R. J. Piechocki, and A. Nix, “Beam alignment for Millimetre wave links with motion prediction of autonomous vehicles,” in *Proc. Antennas Propagat. RF Technol. Transp. Auton. Platforms*, Feb. 2017, pp. 1–8.

[39] I. Orikumhi, J. Kang, C. Park, J. Yang, and S. Kim, “Location-aware coordinated beam alignment in mmWave communication,” in *Proc. 56th Annu. Allerton Conf. Commun. Control, Comput. (Allerton)*, Oct. 2018, pp. 386–390.

[40] N. Garcia, H. Wymeersch, E. G. Ström, and D. Slock, “Location-aided mm-wave channel estimation for vehicular communication,” in *Proc. IEEE 17th Int. Workshop Signal Process. Adv. Wireless Commun. (SPAWC)*, Jul. 2016, pp. 1–5.

[41] H. Chung, J. Kang, H. Kim, Y. M. Park, and S. Kim, “Adaptive beamwidth control for mmWave beam tracking,” *IEEE Commun. Lett.*, vol. 25, no. 1, pp. 137–141, Jan. 2021.

[42] Y. Kang, H. Seo, and W. Choi, “Optimal receive beamwidth for time varying vehicular channels,” in *Proc. IEEE Wireless Commun. Netw. Conf. (WCNC)*, May 2020, pp. 1–6.

[43] E. Park, Y. Choi, and Y. Han, “Location-based initial access and beam adaptation for millimeter wave systems,” in *Proc. IEEE Wireless Commun. Netw. Conf. (WCNC)*, Mar. 2017, pp. 1–6.

[44] Z. Qinghua, C. Ying, S. Junfeng, Z. Jingya, and L. Yong, “Research on beamforming algorithm of millimeter wave system based on mobility of network vehicles,” *J. Phys. Conf. Ser.*, vol. 1939, no. 1, May 2021, Art. no. 12106.

[45] C. Ballesteros, A. Pfadler, L. Montero, J. Romeu, and L. Jofre-Roca, “Adaptive beamwidth optimization under doppler ICI and positioning errors at mmWave bands,” *Veh. Commun.*, vol. 34, Apr. 2022, Art. no. 100456.

[46] C. Perfecto, J. Del Ser, and M. Bennis, “Millimeter-wave V2V communications: Distributed association and beam alignment,” *IEEE J. Sel. Areas Commun.*, vol. 35, no. 9, pp. 2148–2162, Sep. 2017.

[47] Y. Feng, J. Wang, D. He, and Y. Guan, “Beam design for V2V communications with inaccurate positioning based on Millimeter wave,” in *Proc. IEEE 90th Veh. Technol. Conf. (VTC-Fall)*, Sep. 2019, pp. 1–5.

[48] Y. Li, X. Zhang, L. Yan, and D. K. Sung, “An opportunistic routing protocol based on position information for beam alignment in millimeter wave vehicular communications,” in *Proc. IEEE Int. Conf. Commun.*, May 2022, pp. 267–272.

[49] M. Brambilla, L. Combi, A. Matera, D. Tagliaferri, M. Nicoli, and U. Spagnolini, “Sensor-aided V2X beam tracking for connected automated driving: Distributed architecture and processing algorithms,” *Sensors*, vol. 20, no. 12, p. 3573, Jun. 2020.

[50] D. Tagliaferri, M. Brambilla, M. Nicoli, and U. Spagnolini, “Sensor-aided Beamwidth and power control for next generation vehicular communications,” *IEEE Access*, vol. 9, pp. 56301–56317, Apr. 2021.

[51] “Dedicated short range communications (DSRC) message set dictionary,” Soc. Autom. Eng. Int., Warrendale, PA, USA, Nov. 2009.

[52] J. Breu, A. Brakemeier, and M. Menth, “A quantitative study of cooperative awareness messages in production VANETs,” *EURASIP J. Wireless Commun. Netw.*, vol. 2014, pp. 1–18, Jun. 2014.

[53] T. T. Thanh Le and S. Moh, “Comprehensive survey of radio resource allocation schemes for 5G V2X communications,” *IEEE Access*, vol. 9, pp. 123117–123133, Sep. 2021.

[54] “3rd generation partnership project; technical specification group services and system aspects; release 17 description; summary of Rel-17 work items (release 17),” 3GPP, Sophia Antipolis, France, 3GPP TR 21.917 V0.1.0, Nov. 2021.

[55] M. Kok, J. D. Hol, and T. B. Schön, “Using inertial sensors for position and orientation estimation,” *Found. Trends Signal Process.*, vol. 11, pp. 1–153, Nov. 2017.

[56] “Study on evaluation methodology of new vehicle-to-everything (V2X) use cases for LTE and NR,” 3GPP, Sophia Antipolis, France, 3GPP TR 37.885 V15.3.0, Jun. 2019.

[57] W. B. Heard, *Rigid Body Mechanics: Mathematics, Physics and Applications*. Hoboken, NJ, USA: Wiley, Dec. 2005.

[58] Z. Wei, D. W. K. Ng, and J. Yuan, "NOMA for hybrid mmWave communication systems with beamwidth control," *IEEE J. Sel. Topics Signal Process.*, vol. 13, no. 3, pp. 567–583, Jun. 2019.

[59] S. J. Orfanidis. "Electromagnetic waves and antennas." 2016. [Online]. Available: http://eceweb1.rutgers.edu/~orfanidi/ewa/

[60] C. A. Balanis, *Antenna Theory: Analysis and Design, 4th Edition*. Hoboken, NJ, USA: Wiley, Feb. 2016.

[61] *Study on Evaluation Methodology of New Vehicle-to-Everything (V2X) Use Cases for LTE and NR*, 3GPP, Sophia Antipolis, France, Jun. 2019.

[62] "WGS 84 implementation manual," Eur. Org. Safety Air Navigat., Instit. Geodesy Navigat., Brussels, Belgium, Feb. 1998.

[63] G. Ciaramitaro et al., "On the impact of road roughness and antenna position on vehicular communications," *IEEE Wireless Commun. Lett.*, vol. 11, no. 9, pp. 1875–1879, Sep. 2022.

[64] *Mechanical Vibration—Road Surface Profiles—Reporting of Measured Data*, Int. Org. Standard., Geneva, Switzerland, Nov. 2016.

[65] "Intelligent transport systems (ITS); vehicular communications; basic set of applications; part 2: Specification of cooperative awareness basic service," ETSI, Sophia Antipolis, France, ETSI EN 302 637–2 V1.3.1, Sep. 2014.

[66] "Intelligent transport systems (ITS); users and applications requirements; part 2: Applications and facilities layer common data dictionary," ETSI, Sophia Antipolis, France, ETSI TS 102 894–2 V1.2.1, Sep. 2014.

[67] Y. Feng, D. He, Y. Guan, Y. Huang, Y. Xu, and Z. Chen, "Beamwidth optimization for millimeter-wave V2V communication between neighbor vehicles in highway scenarios," *IEEE Access*, vol. 9, pp. 4335–4350, Jan. 2021.

GIOVANNI CIARAMITARO (Graduate Student Member, IEEE) received the B.Sc. degree in mechanical engineering and the M.Sc. degree in automation and control engineering from the Politecnico di Milano, Milan, Italy, in 2017 and 2020, respectively, where he is currently pursuing the Ph.D. degree in information technology. His main research topics include automotive navigation and sensor fusion to support vehicle-to-everything communication and sensing for connected-automated driving. He was the recipient of the Best Thesis Award at the 2019 Huawei Italy University Challenge (3rd prize).

MATTIA BRAMBILLA (Member, IEEE) received the B.Sc. and M.Sc. degrees in telecommunication engineering and the Ph.D. degree (cum laude) in information technology from the Politecnico di Milano, Milan, Italy, in 2015, 2017, and 2021, respectively. He was a Visiting Researcher with the NATO Centre for Maritime Research and Experimentation, La Spezia, Italy, in 2019. In 2021, he joined the Faculty of Dipartimento di Elettronica, Informazione e Bioingegneria, Politecnico di Milano as a Research Fellow. His research interests include signal processing, statistical learning, and data fusion for cooperative localization and communication. He was the recipient of the Best Student Paper Award at the 2018 IEEE Statistical Signal Processing Workshop.

MONICA NICOLI (Senior Member, IEEE) received the M.Sc. (Hons.) and Ph.D. degrees in communication engineering from the Politecnico di Milano, Milan, Italy, in 1998 and 2002, respectively. She was a Visiting Researcher with ENI Agip from 1998 to 1999, and Uppsala University, Uppsala, Sweden, in 2001. In 2002, she joined the Politecnico di Milano as a Faculty Member, where she is currently an Associate Professor of Telecommunications with the Department of Management, Economics and Industrial Engineering. Her research interests include signal processing, machine learning, and wireless communications, with emphasis on smart mobility and Internet of Things applications. She was the recipient of the Marisa Bellisario Award in 1999 and a co-recipient of the Best Paper Awards of the IEEE Symposium on Joint Communications and Sensing in 2021, the IEEE Statistical Signal Processing Workshop in 2018, and the *IET Intelligent Transport Systems Journal* in 2014. She was an Associate Editor of the *EURASIP Journal on Wireless Communications and Networking* from 2010 to 2017 and a Lead Guest Editor of the Special Issue on *Localization in Mobile Wireless and Sensor Networks* in 2011. She is an Associate Editor of IEEE TRANSACTIONS ON INTELLIGENT TRANSPORTATION SYSTEMS.

UMBERTO SPAGNOLINI (Senior Member, IEEE) is a Professor of Statistical Signal Processing, the Director of Joint Lab Huawei-Politecnico di Milano, and the Huawei Industry Chair of the Politecnico di Milano. His research in statistical signal processing covers remote sensing and communication systems with more than 380 papers on peer-reviewed journals/conferences and patents. He is the author of the book *Statistical Signal Processing in Engineering* (J. Wiley, 2017). He is the Technical Expert of standard-essential patents and IP. His research interests include mmW channel estimation and space-time processing for single/multiuser wireless communication systems, cooperative and distributed inference methods, including V2X systems, mmWave communication systems, parameter estimation/tracking, focusing and wavefield interpolation for remote sensing (UWB radar and oil exploration), and integrated communication and sensing. He was the recipient/co-recipient of the Best Paper Awards on Geophysical Signal Processing Methods (from EAGE), the Array Processing (ICASSP 2006), the Distributed Synchronization for Wireless Sensor Networks (SPAWC 2007, WRECOM 2007), the 6G Joint Communication and Sensing (JC&S 2021), and the SAR Imaging for Automotive (MMS 2022). He served as a part of IEEE editorial boards as well as a member in technical program committees of several conferences for all the areas of interests.

Open Access funding provided by 'Politecnico di Milano' within the CRUI CARE Agreement